

Integration of ASTER and airborne geophysical data for mineral exploration and environmental mapping: a case study, Gabal Dara, North Eastern Desert, Egypt

Kh. Gemal¹ · N. M. Abd-El Rahman² · B. M. Ghiath³ · R. N. Aziz³

Received: 4 August 2015 / Accepted: 13 January 2016 / Published online: 29 March 2016
© Springer-Verlag Berlin Heidelberg 2016

Abstract Remote sensing ASTER-SWIR data and airborne geophysical techniques are cost effective and accurate mapping tools for mineral exploration and environmental mapping, compared with the conventional geological methods. In the present work, the ASTER data, airborne gamma ray spectrometry and magnetic techniques were applied for mapping alteration and/or mineralization zones in the granitic rocks of Gabal Dara area. In addition, the natural dose rate was calculated and compared with stream networks and structural lineaments to define the potential hazards caused by anomalous distribution of natural radioelements. In Gabal Dara area, Syeno-granite unit was considered as a mapping target due to the high concentration of radioactive materials as indicated from gamma-ray spectrometry data. Remote sensing techniques and airborne geophysical data analysis through GIS based modeling were jointly applied in a mineral exploration context to identify radioactive rich potential areas in the considered area. The obtained results illustrate the efficiency of the integrated methodological approach as an effective tool to provide information on alteration minerals which are valuable for mineral exploration activities and support the role of ASTER VNIR-SWIR and airborne

geophysical data integration as a very effective tool and robust image processing technique for that purpose. The constructed vector maps can be used as a guide for further follow-up of radioelement and mineral exploration works and for environmental monitoring in the area.

Keywords Principal component · Gamma-spectrometry · Alteration zones · Natural radiation · Dose rate

Introduction

The use of remote sensing technology and airborne geophysical techniques in geological mapping and mineral exploration has been very successful in pointing out the presence of alteration minerals such as chlorite, kaolinite, sericite, hematite and illite, which are important in the identification of hydrothermal alterations and radioactive mineralization. In addition, integration of these techniques is helpful in identification and delineation of various land forms, flood hazards, lineaments and structural elements which are related to environmental mapping (Javed and Wani 2009). Alteration in the form of anomalous clay and other minerals (illite, kaolinite, chlorite), and geochemical enrichment in uranium and pathfinder elements, tend to form haloes in the overlying rocks, which are useful in exploring for buried deposits (Boyer 1979; Berger and Henley 1989; Cuney 2009). These mineral assemblages and other minerals are common in the granitic massive of Gabal Dara area in the Egyptian Eastern Desert which is considered as a case study in the present work (Fig. 1).

A cooperation effort between NASA and Japan's Ministry of Economic Trade and Industry (METI) has yielded a sensor, known as the Advanced Spaceborne Thermal Emission Reflection Radiometer (ASTER). ASTER is an

✉ Kh. Gemal
khaledgemal@zu.edu.eg

¹ Environmental Geophysics Laboratory (ZEGL), Geology Department, Faculty of Science, Zagazig University, Zagazig 44519, Egypt

² Geological Applications and Mineral Resources Division, National Authority for Remote Sensing and Space Sciences, Cairo, Egypt

³ Exploration Division, Follow Up Department, Egyptian Nuclear Materials Authority, Cairo, Egypt

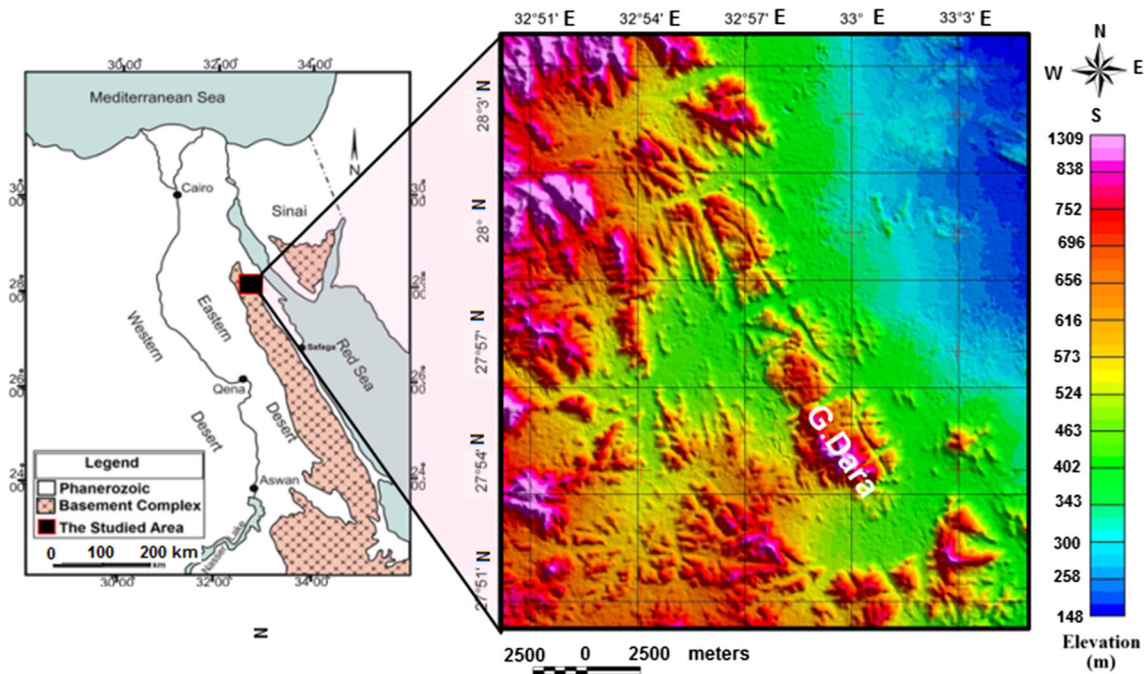


Fig. 1 Base and shaded color topographic maps of Gabal Dara area, Eastern Desert, Egypt

advanced multispectral imager covering a wide spectral range (14 bands) from the visible near infrared (VNIR) to the thermal infrared (TIR) of electromagnetic spectrum. VNIR-SWIR (nine bands) spectral analysis techniques have been successfully applied for mapping and discriminating lithologic units and hydrothermal alteration pattern in well exposed areas as in the present case study (Rowan and Mars 2003). Spectral identification of potential areas of hydrothermal alteration minerals is a common application of ASTER to mineral exploration. The extraction of spectral information related to this type of target from Landsat Thematic Mapper (TM) imagery has been achieved through the use of image processing techniques such as band ratio and principal component analysis, PCA (Sabine 1999; Crosta et al. 2003). ASTER channels are more continuous in the short wave infrared region than those of Landsat (Gupta 2003; Zhang et al. 2007), which increase their accuracy in the spectral identification of rocks and minerals (Crosta et al. 2003). For this reason, the ASTER data are more advanced compared with other sensors for lithological mapping (Carranza and Hale 2002; Gad and Kusky 2006, 2007; Zhang et al. 2007; Raharimahefa and Kusky 2009; Elsaid et al. 2014; Bharti and Ramakrishnan 2015).

Alternatively, airborne gamma-ray spectrometry and magnetic data can be used as one of the powerful tools in geological mapping, especially in areas of high terrain complexity. The conventional approach to the acquisition

and processing of airborne gamma-ray spectrometric data is to monitor three relatively broad spectral windows (IAEA 2003). These three elements are used for the measurement of K, U and Th concentrations. Additionally, the total count window (TC) gives a measure of the total radioactivity. In the anomalous radioactive areas, the radioactivity of soils is essential for understanding changes in the natural radiation background (Sroor et al. 2001; Chiozzi et al. 2002). The natural radioactivity of soil and sediment depends on the soil and sediment formation and transport processes.

The integration of ASTER satellite data analysis, airborne gamma-ray spectrometric and magnetic techniques is fast and economic methods that have been used in environmental mapping and mineral exploration (Daviz and Guilbert 1973; Crowley et al. 1989; Rowan et al. 1996; Minty and FitzGerald 2015). In the present work, the ASTER and airborne gamma-ray spectrometric and magnetic data are used and integrated for mapping mineralogical patterns and radioactive mineralization zones in Gabal Dara area, Eastern Desert of Egypt (Fig. 1). Principal component analysis (PCA) and feature oriented principal component selection (FPCS) were applied to ASTER bands covering the SWIR with the objective of mapping the occurrence of alteration end members related to the obtained radioactive anomalous zones from gamma-ray spectrometric data. The surface lineaments extraction from space images was carried out and integrated with

subsurface lineaments from magnetic data to outline the alteration zones in the area. Radioactive distributions, lineaments, and alteration zones were used as control factors to construct a vector model which can be used as a guide for further follow-up radioelement and mineral exploration works in the area.

In addition, the exposure rate and dose rate values were determined using airborne gamma-ray spectrometric data and compared with active drainage basins and structural lineaments to study the environmental impact of natural radiation and understanding of the potential hazards caused by anomalous distribution of natural radioelements.

Geological background

Gabal Dara area is situated, in the North Eastern Desert of Egypt between latitudes 27°50'N and 28°05'N and longitudes 32°50'E and 33°05'E. It is essentially composed of Younger (pink) Granites. Gabal Dara possesses an oval shape, which represents an elongated belt of about 28 km in length and an average width of about 25 km, trending N–S direction and occupies an area of approximately 700 km² (Fig. 1).

Gabal Dara area is dominated by presence of both igneous and metamorphic rocks of the basement complex, with the exception of its northeastern corner, which is mainly covered by sedimentary rocks. The exposed rocks belong mostly to the Late Precambrian, early passing to early Paleozoic, except the Phanerozoic Volcanics which are Mesozoic age. These rocks are traversed by several wadis filled with Quaternary alluvial deposits (El Shazly 1977).

The basement complex of the Precambrian age is represented by Metavolcanics, Metagabbro, Older Granitoides, Younger Granites and Phanerozoic cover of Nubian Sandstones and alluvial deposits. Figure 2 illustrates the surface geologic map of Gabal Dara area. This map was reconstructed after Conoco Coral and Egyptian General Petroleum Corporation, (EGPC 1987) by refreshing colors and clarifying the geologic rock units.

The Younger Granites (Ga, Fig. 2) form the main masses of Gabal Dara and considered as target for mapping process in the present study. These granites are strongly controlled by some major structures especially the NNW–SSE fault system which is parallel to the Gulf of Suez trend (Shalaby 1985). The pink granites in Wadi Dara are medium to coarse grained and composed of orthoclase, plagioclase feldspars, quartz, biotite and rare hornblende.

Abd-Elmoneim et al. (1988) studied the geology and radioactivity of Gabal Dara area. They mentioned that the area is essentially composed of younger granites. The marginal parts of Gabal Dara are characterized by the

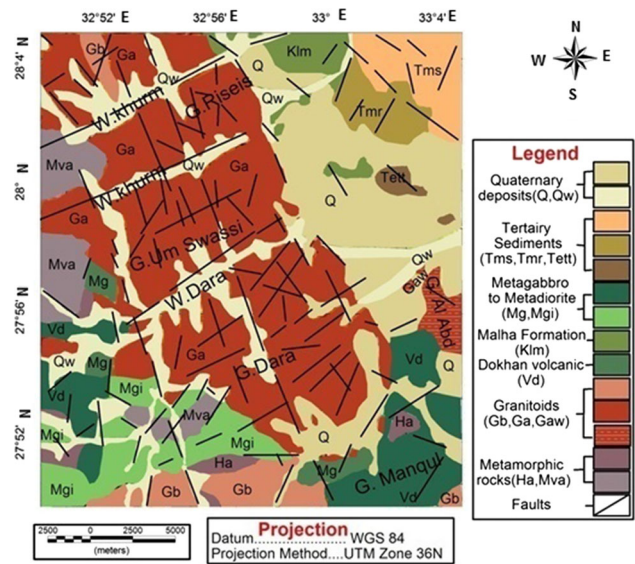


Fig. 2 Compiled geologic map of Gabal Dara area (Conoco and EGPC 1987)

presence of numerous pegmatite bodies in which several radioactive anomalies were recorded. The radiometric and metallographic studies indicate that the high radioactivity mainly of pegmatite bodies is mainly due to the presence of euxenite mineral gains. In Gabal Dara area, the considerable parameters of the mineralized zones of veins and veinlets make it possible to recommend the ore occurrence for more detailed investigations using geophysical and remote sensing data.

ASTER and geophysical data

Remote sensing ASTER data

The ASTER raw data are a raster file composed of a series of layered data points across a grid that spans nearly about 4500 km². Two scenes were used to cover Gabal Dara area and its surroundings. Each ASTER scene covers an area of 60 × 60 km². The visible–near infra-red (VNIR) bands have a spatial resolution of 15 m, the short wave infra-red (SWIR) bands have a spatial resolution of 30 m and the thermal infra-red (TIR) bands have a spatial resolution of 90 m. The selected two ASTER scenes (level 1B) were acquired in 15 May 2001. These scenes were treated by several levels of pre-processing and enhancement techniques such as atmospheric correction (FLAASH), and mosaicking images. Radiometric corrections were applied for ASTER data. Radiometric contributions from the Earth’s atmosphere were removed to isolate the effect from rock (Scheidt and Lancaster 2008; Matar and Bamousa 2013).

The analysis of ASTER VNIR-SWIR bands data in the present work aims to identify and separate the Younger Granite then mapping the alteration minerals to define relationship between the high concentrations of radioelements and common alteration end members in this rock unit. To achieve this goal, false color composite (FCC) image and principal component analysis (PCA) techniques were applied as the following.

Color composites image

The difference in energy levels within a single band (gray scale) may not be obvious. So, comparing of spectral characteristics of land features in multiple bands (color composites) gives a better separation or contrast between different land surfaces when displayed as red green blue (RGB). Color composite images have been constructed using combination three bands. The production of color composite images based on known spectral properties of rocks and alteration minerals in relation to the selected spectral bands. Unlike the landsat ETM+ image, ASTER does not have a real blue band and therefore, the created RGB image does not look like a true-color image. To create a color composite image of the area, the Optimum Index Factor (OIF) was applied to select the optimum combination of three bands in a satellite image using ILWIS Open software. The best combination for lithological mapping is selected from the highest ranking OIF calculated value. Figure 3 shows false color composite (FCC) image of three bands (1, 2 and 9 with average wavelengths 0.54, 0.66 and 2.395 μm , respectively) at the highest OIF index. The selected FCC image clearly illustrates the rock units of the area and correlate with the pre-mentioned geologic mapping (Fig. 2). In this image, the Younger Granites could be easily identified forming the main body of Gabal Dara.

Principal component analysis (PCA)

The principal component transformation is a multivariate statistical technique widely used in image processing for geological mapping that transforms a number of correlated spectral bands into a smaller number of uncorrelated spectral bands called principal components (Singh and Harrison 1985; Loughlin 1991; Vincent 1997). Therefore, principal component transformation (PC) helps to enhance and separate certain types of spectral signatures from the background (Ghulam et al. 2010). It is a well-known method for lithological and alteration mapping in metallogenic areas (Crosta et al. 2003).

The PC-transformation was calculated for the VNIR-SWIR nine bands then the PC3, PC2 and PC1 as red, green and blue composite image of the area was created as shown

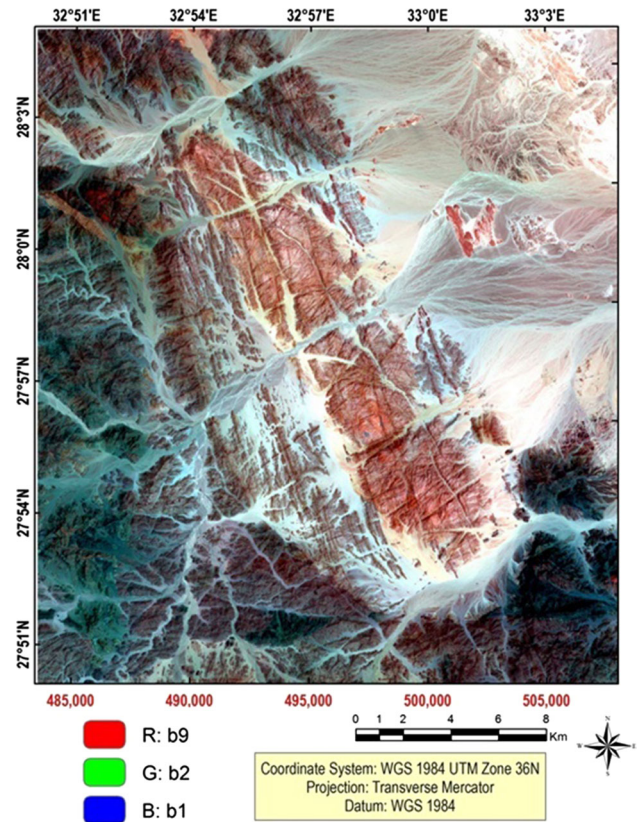


Fig. 3 False color composite, FCC image of bands 9, 2, 1 as R, G, and B of OIF rank 2

in Fig. 4. Such image successfully discriminates and characterizes the younger granites of Gabal Dara by the red to pink colors, Monzo-granite by bluish green color, older granitoides by pale violet color, metavolcanics by pale blue color, Hamammat sediments bright color, Dokhan volcanics by pale green color, Tertiary Sediments by dark green color and Quaternary Sediments by black color.

Airborne gamma-ray spectrometric data

In 1984, cooperation between the Egyptian General Petroleum Corporation, the Egyptian Geological Survey and Mining Authority and Aero-Service Division, Western Geophysical Company of America was formed, which include an airborne magnetic and spectral gamma-ray survey over a huge part of the Eastern Desert of Egypt. Gabal Dara and its surroundings was a part of this survey (Aero-Service 1984). The traverse lines took N45°E direction, with a spacing of 1.5 km approximately (Fig. 5). The tie lines were perpendicular to the traverse lines (N135°E direction) and spaced about 10 km. High-sensitivity 256-channel (12 keV/channel) gamma-ray spectrometer system was used with two detector systems for measuring the terrestrial radiation and the atmospheric radon.

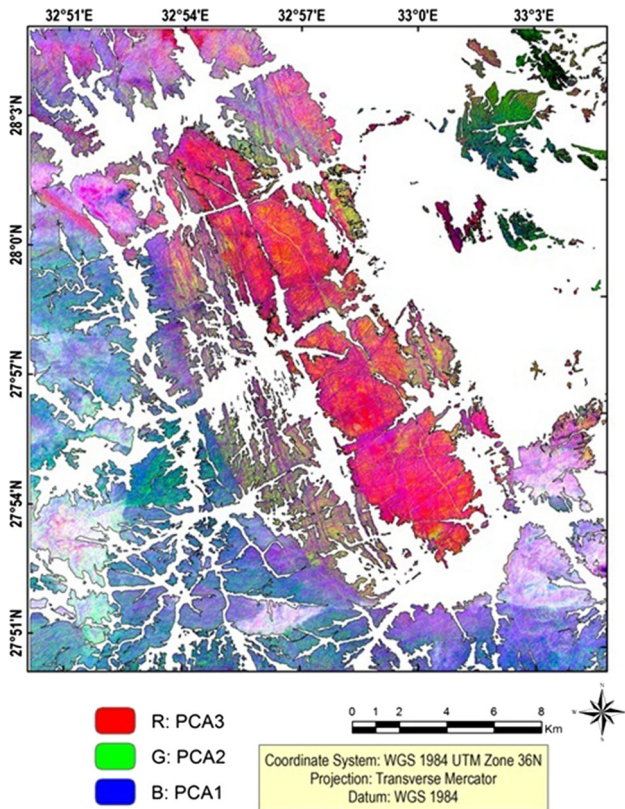


Fig. 4 PCA3, PCA2, and PCA1 as R, G, and B composite image of the study area using the nine ASTER VNIR-SWIR bands

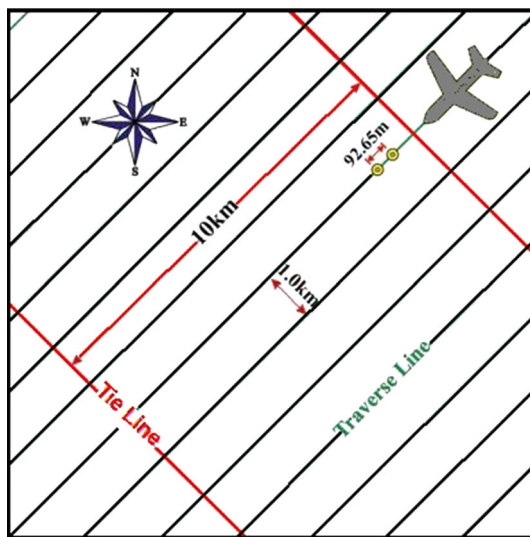


Fig. 5 Flight path of the airborne gamma-ray spectrometry of Gabal Dara area (Aero-Service Report 1984)

Data processing includes two main categories such as: sources of error and correction of spectral radiometric data. The first one consists of scattering effects, background effects, and atmospheric effects. On the other side the second one, contain background effects, stripping ratio,

altitude correction and finally conversion to apparent radiometric concentration.

Airborne spectral radiometric surveying of Gabal Dara area provides valuable information for four parameters (variables) namely: total-count of the gamma radiation (TC, in $\mu\text{R/h}$), absolute concentrations of the three radioelements: potassium (K40, in %), equivalent uranium (eU, in ppm) and equivalent thorium (eTh, in ppm).

Figure 6 shows the spatial distributions and concentrations of radioelements of Gabal Dara area. In these maps, the boundaries of the Younger Granites can be easily delineated due to the high concentration of radioelements. On the other hand, all spectrometric maps illustrate the boundaries of younger granites and other geological formations are characterized by low values of natural radioelement abundances. The major trend that could be traced from the four radiometric maps is the NW trend at Gabal Dara which is considered as anomalous area compared with other rock types.

The total count map (Fig. 6a) shows three major general levels of radiation, the high level (level 3 ranges from 9.5 to 19 $\mu\text{R/h}$) and is represented by the orange, red and magenta colors; this range is correlated mainly with the granitoid rocks (Ga and Gaw in the geological map of Fig. 2). The intermediate level (level 2 from yellow to bright green is ranging from 6 to 9.5 $\mu\text{R/h}$) and is represented by the green color to yellow. This range is correlated with the Quaternary alluvial soils which received huge amounts of annual floods through active drainage networks crossing the anomalous granitic massive of Gabal Dara. The lowest level in the northeastern corner ranges from 2 to 6 $\mu\text{R/h}$ represents Tertiary Sediments with the pale blue to green color.

Potassium, Uranium and Thorium maps (Fig. 6b–d) show great similarity with the total count map (Fig. 6a) where the younger granite represents a clear anomalous area. The concentration values in level ranges from (0.3, 3.6 %), (1.1–10.5 ppm eU) and (1.2–30.9 ppm eTh) for potassium, uranium and thorium maps, respectively (all values are multiplied by 10 to show relative variation of the gamma radiation).

Airborne magnetic data

In the airborne magnetic survey, a Varian V-85 proton free-precession magnetometer was used with a sensitivity of 0.1 nT. The base station magnetometer was a Varian VIW 2321 G4, single cell cesium vapour (Aero-Service 1984). The magnetic measurements were subjected to diurnal and International Geomagnetic Reference Field corrections to drive the magnetic anomalies. The magnetic anomalies do not appear vertically over the targets and are asymmetrical in nature due to the dipole nature of magnetic field and

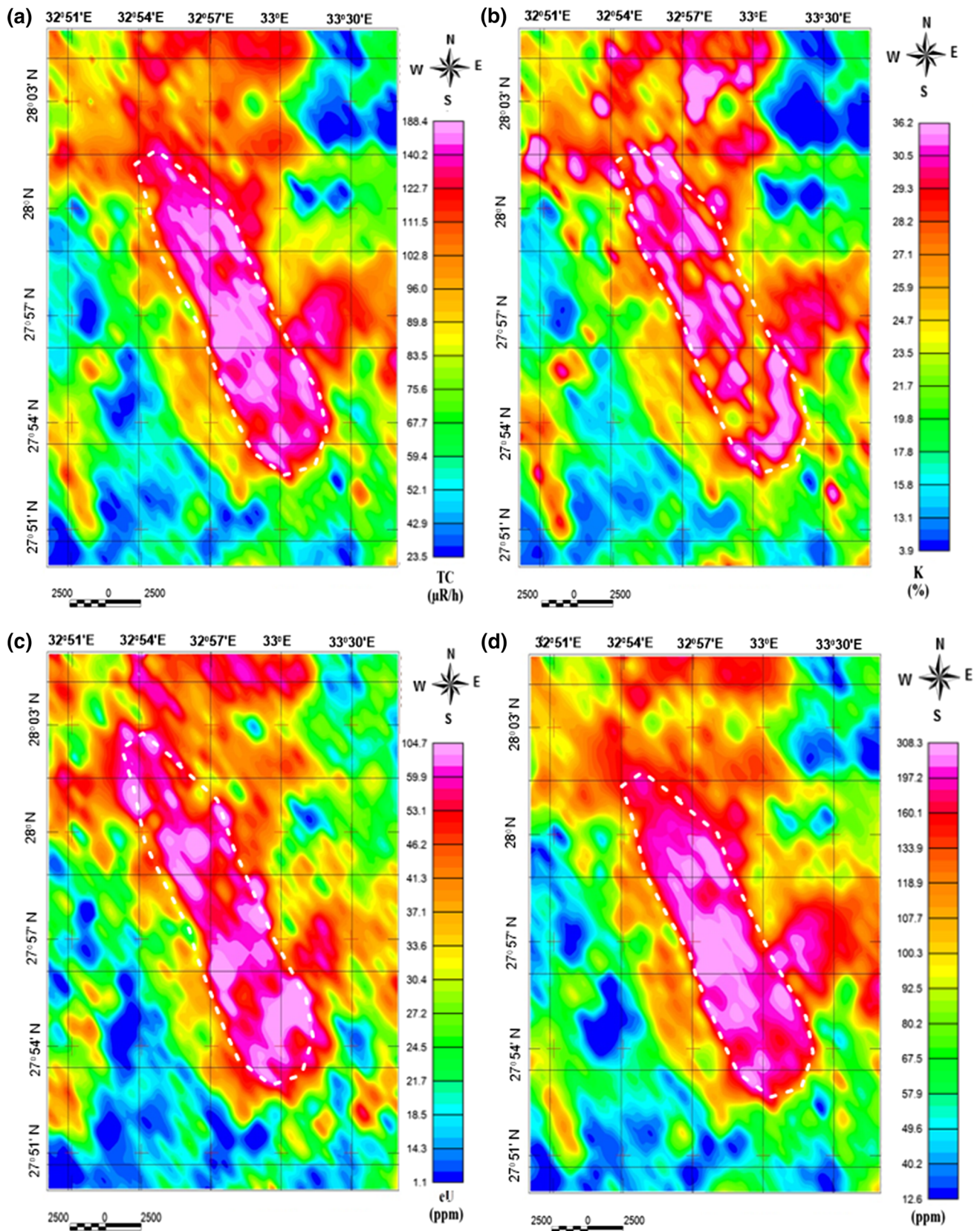


Fig. 6 Spatial distributions and concentrations of radioelements of Gabal Dara area: **a** total count (TC in $\mu\text{R/h}$), **b** potassium (K; in %), **c** equivalent uranium (eU, in ppm), **d** equivalent thorium (eTh; in ppm). All values are multiplied by 10

inclination–declination of Earth’s magnetic field. These distortions in magnetic anomalies were removed using reduction-to-pole (RTP) method.

The total magnetic field and RTP magnetic maps (Fig. 7) show clearly three distinct zones. The first zone is located around Gabal Dara and characterized by high magnetic amplitude with NW–SE trend. As shown from the geologic map (Fig. 2), this zone is conjugated with the older granite and metamorphic rocks of Gabal Dara area. The second zone encountered in the middle side of the study area. It is characterized by low magnetic amplitude with oval shape NW–SE trend. This zone represents the younger granite of Gabal Dara, Gabal El Ein and Gabal Riseis. Finally, low magnetic values occur in the northeastern parts where lithologies belonging to sedimentary cover. These observations may suggest that most of the basement rocks in area are either outcropping or extend to shallow depths.

In the RTP aeromagnetic map (Fig. 7b), the magnetic anomalies are frequently related to fractures and align themselves along definite axes forming trends. In other words, the structural conditions of the area are reflected significantly in the pattern, trends and intensities of magnetic anomalies appearing on aeromagnetic map. In this case, trend analysis is an extremely significant technique in the interpretation of geological features and mineralization zones of Gabal Dara area. This method of analysis could

reveal the directions (trends) of forces and their strengths, as well as the mineralization emplacement and control. Hence, in primary stages, mapping geologic lineaments are important as long-range management for mineral exploration, because of their potentials for harboring ore bodies that are carried and deposited by ascending hydrothermal fluids (Feizi and Mansouri 2013).

Near surface and deep seated structural lineaments were detected from anomalies of the residual and regional magnetic-component maps, respectively (Fig. 8). In addition, the surface lineaments were automatically extracted from ASTER- Global Digital Elevation Model V2 (ASTER GDEM V2) data using the PCI Geomatica software, lineament extraction algorithm (PCI Geomatica 2013) as shown in Fig. 9. ASTER GDEM has 15 m horizontal spatial resolution where each scene consists of 4100 samples by 4200 lines, corresponding to about 60 km-by-60 km ground area. Vertical accuracy is specified 95 % confidence level with 20 m varying between 10 and 25 m (ASTER GDEM Validation Team 2009).

The obtained results from magnetic and ASTER GDEM techniques show a good correlation. The directional analysis of the automatically extracted lineament maps revealed that NW–SE, NNW–SSE, E–W and N–S (in descending manner) are common trends in the area, besides NE–SW and NNE–SSW as a minor faulting trend.

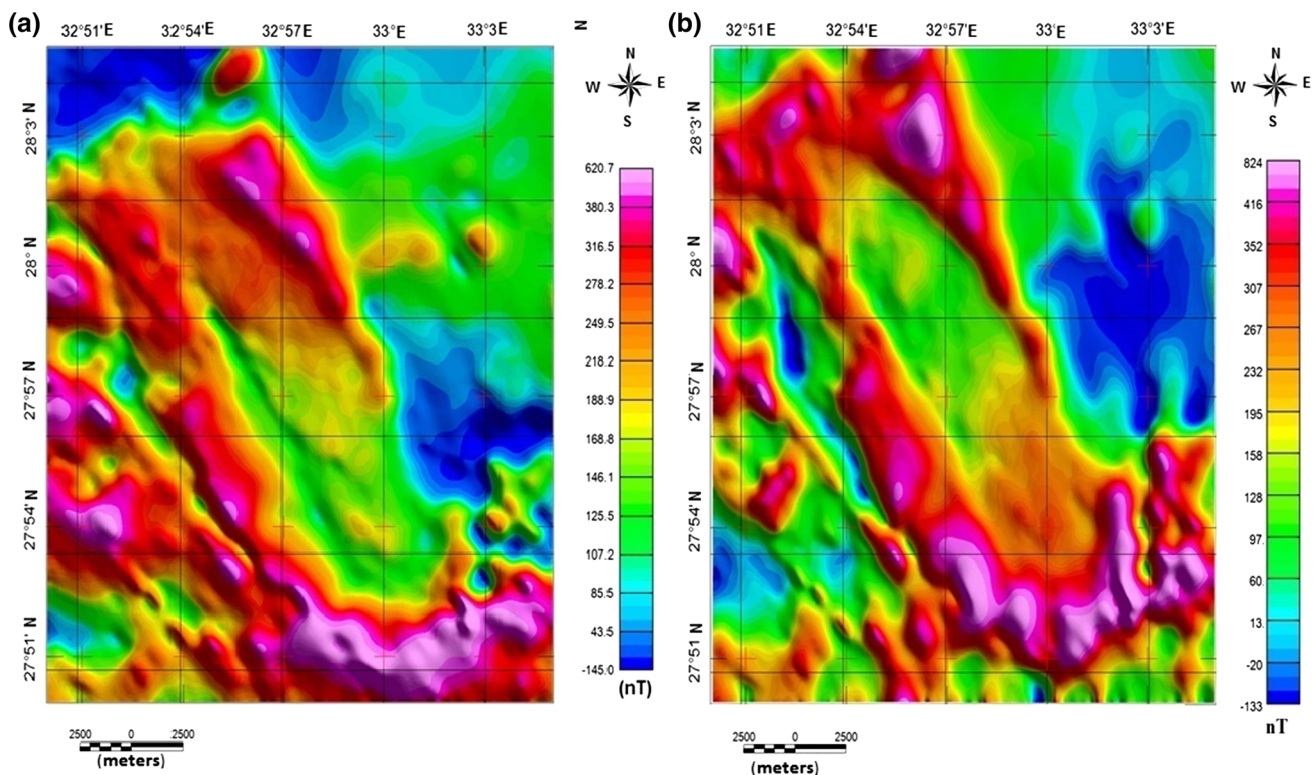


Fig. 7 Shaded color map of **a** total magnetic field and **b** reduced to North Pole (RTP) of total magnetic intensity field, Gabal Dara area

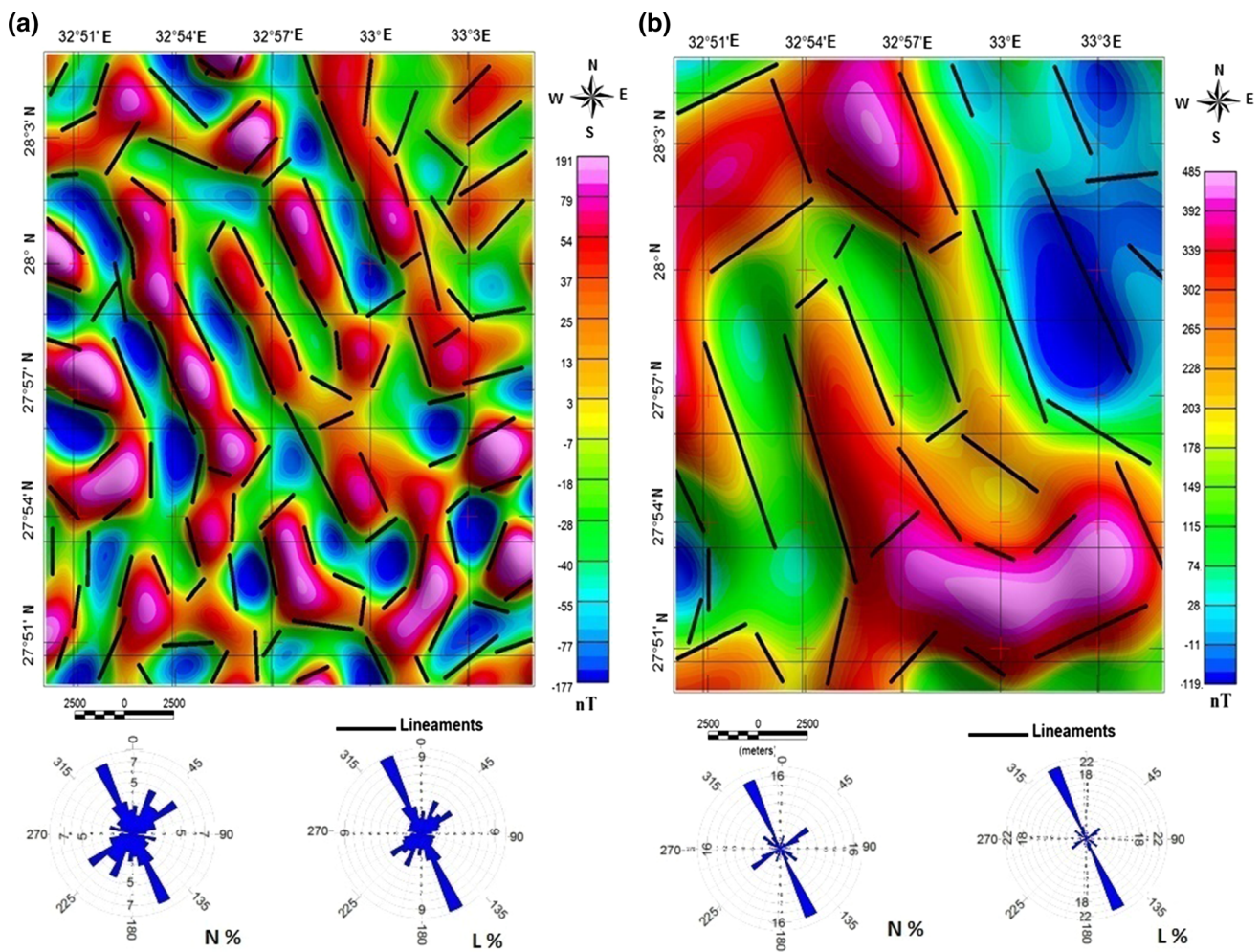


Fig. 8 Interpreted lineaments and directional analysis (*rose diagram*) of lineament frequencies (*N %*) and lineament lengths (*L %*) **a** deep-seated lineaments as extracted from regional magnetic component map and **b** shallow lineaments as extracted from residual magnetic component map

Data analysis and discussion

Mapping of mineralization zones

The radioelement mineralization is controlled by the abundance of some alteration minerals (e.g., hematite, illite, seircite and chlorite) and the lineaments including factures and deep seated faults where these lineaments are considered as suitable pathways for mineralizing solutions (Cuney 2009). To understand the significance of these controlling factors on the radioactive mineralization in the granitic pluton of Gabal Dara, the lineaments, common endmember alteration minerals and radioactive abundance maps were used to construct a mineralization model of the anomalous radioactive granites as shown in Fig. 10. To construct to this model, the converting of VNIR-SWIR was used to identify the primary end member alteration minerals including chlorite, kaolinite, illite, alunite, epidote, seircite, quartz, montmorillonite and hematite. The

constrained energy minimization (CEM) technique was used to detect the abundance of the alteration minerals using ASTER resampled Jet Propulsion Laboratory (JPL) spectral library covering VNIR-SWIR spectral region. In addition, structural lineaments from the aeromagnetic data (residual and regional) were used with the abundance radioelement maps (K%, eU and eTh). This model is integrated in the variety of layers or employing combination of multi-source data to derive particular set of observables used in target detection. These favorable factors for radioactive mineralization are used as input layers to create the GIS based model and the considered area classified using ArcGIS 10.2 software.

According to this integrating approach, four new sites were suggested for uranium exploration, which have similar conditions as the explored sites at Gabal Dara area. The suggested sites are characterized by combinations of hematite (oxidized minerals), kaolinite, illite and chlorite with maximum radioactivity concentration and the highest

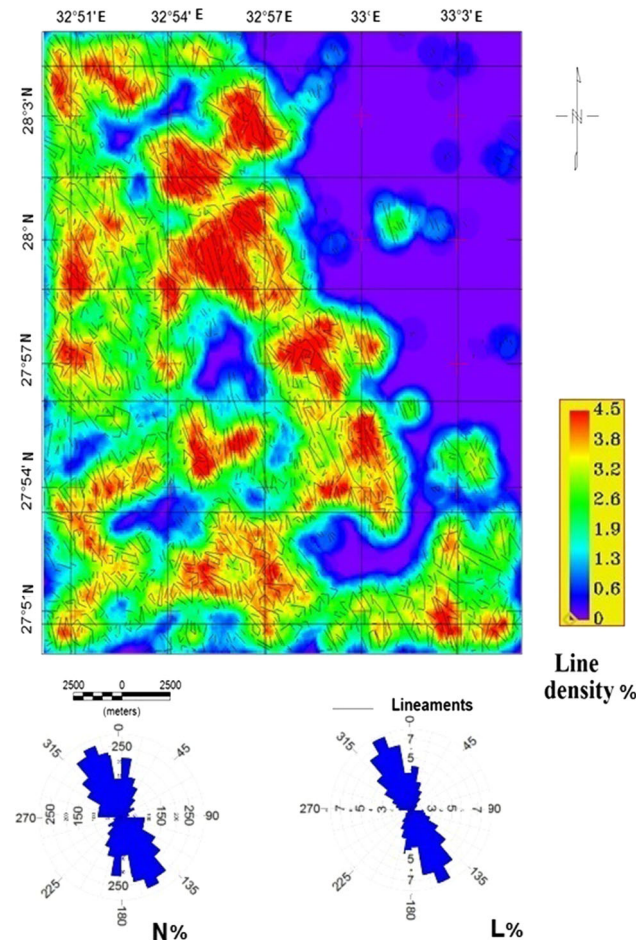


Fig. 9 Surface lineaments automatically extracted from ASTER GDEM data and directional analysis (*rose diagram*) of lineament frequencies (*N %*) and that of lineament lengths (*L %*)

density of NW–SE faults/lineaments which are considered as favorable trends for structural guided radioactive mineralization in the area. According to Brooknis (1982) and Yu et al. (2010), these zones are favorable regions for hydrothermal activities and altered radioactive mineralization. Two sites at the north have high concentration of kaolinite, montmorillonite with hematite and also have the maximum account of radioelements at NW–SE major trend. The middle site has high amount of radioelements and high concentration of hematite with combination of kaolinite and chlorite. Finally, the southern site has hematite with sericite as a phyllic alteration zone and high concentration of radioactivity. The Nuclear Materials Authority (NMA) of Egypt conducted a comprehensive exploration program in the southern site due to its priority for radioactive mineralization based on the field observations.

The obtained model yields the highest score in the quantity and usability of airborne data collected. However, further detailed ground gamma ray spectrometric

measurements along with mineralogical and geochemical studies should be integrated with higher spectral resolution imagery (like hyper spectral data) to delineate the mineralogical patterns of the suggested sites. Without any ground surveys, the alteration mineral images are only a qualitative representation of the true composition of the area.

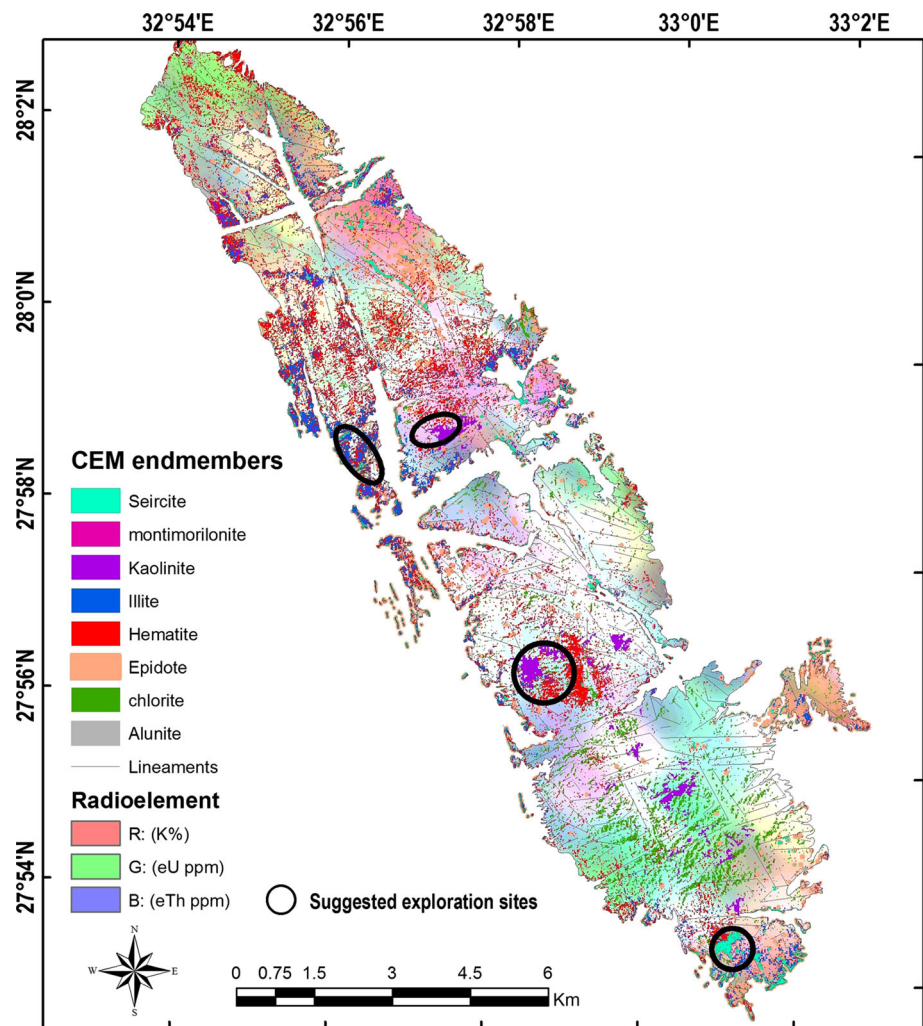
Environmental mapping

In the radioactive anomalous zones such as in the granitic pluton of Gabal Dara and its surroundings, the radioactive minerals may occur either as residual or secondary deposits in soils and tend to concentrate with coarse gravel in streams, and in black sands on Gulf of Suez coast. Secondary deposits form due to the leaching of uranium from minerals during chemical weathering where uranium is mobile in groundwater and floods.

As indicated from geological map and composite images, the anomalous granites in Gabal Dara are drained by several streams such as Wadi Dara, Wadi Malaha and Wadi Khorum. As shown in Fig. 11, these basins represent separate drainage systems, which are active during rainy periods in winter and fall. These basins flowing through the alluvial plain of the area up the Gulf of Suez coast near Ras Shokeir area, where there are many developing activities, petroleum constructions and other industrial sites. Based on flood hazard analysis and vulnerability map of the area, Wadi Khorum and Wadi Karim in the northern parts were classified as highly vulnerable for flood hazard and Wadi Dara in the middle part is moderately flood hazard (Youssef and Hegab 2005). These drainage systems are structurally controlled and buried in the eastern sedimentary plain towards the Gulf of Suez coast. The eastern sedimentary plain receives a great amount of annual floods coming from these drainage systems and passing through the anomalous radioactive zones in Gabal Dara. In such environment, the radioactivity of soils and groundwater in the coastal plain is essential for understanding changes in the natural radiation background.

The exposure rate and dose rate values were calculated using airborne gamma-ray spectrometric data. The natural radiation (exposure rate) is frequently referred to as a standard for comparing additional sources of man-made radiation such as atomic weapon fallout, nuclear power generation, radioactive waste disposal, etc. To understand the vulnerability of natural radiation levels in the area, the drainage networks were set in background of the calculated dose rate map and presented in Fig. 11. The mean natural dose rates computed from the terrestrial gamma-radiation range from 0.2 to 1.6 mSv/year. The dose rate levels still remain in the safe side (<1 mSv/year according to UNSCEAR 1988; IAEA 2005) and within the maximum permissible safe radiation dose rate without harm to the

Fig. 10 CEM classified end members and lineaments overlying radioelement ternary image



individual except the high vulnerable zone of younger granites (1.2–1.6 mSv/year) and fan of Wadi Khorum in the northern parts as well as the some tributaries in the middle part (Fig. 11). This high vulnerable zone should be subjected for further follow up investigations to assess the land and water uses and a dose monitoring program is necessary. On the other hand, the alluvial fans of Wadi Dara main stream and Wadi Malaha in the alluvial plain represent low to moderately vulnerability between 0.7 and 1.2 mSv/year.

Conclusions

The granitic rocks in Gabal Dara, Egyptian Eastern Desert are characterized by anomalous concentration of radioactive elements. The analysis of airborne gamma-ray spectrometry and magnetic data aided to trace the anomalous granitic pluton of Gabal Dara (Syeno-granite), which is characterized by relatively high concentrations of

radioactive materials as Tc, eU, eTh, and K. The concentration values in the area is varied from 9.5 to 19 μ R/h, 2.8 to 3.6 %, 4.6 to 10.5 ppm eU, and 12.5, 30.9 ppm eTh for total count, potassium, uranium and thorium maps, respectively.

Application of several image processing methods to ASTER data allows to distinguish the lithologic and abundance of alteration minerals on the ground. FCC image, PCA and CEM methods were applied on the ASTER data to map the considered anomalous radioactive granitic rocks. The applied techniques showed results considered satisfactory with gamma-ray spectrometry and magnetic maps.

In the present study, the analysis of ASTER data presents an approach to extract the alteration distribution information in granitic massive of Gabal Dara for uranium exploration and environmental mapping. Results indicate that ASTER and the integration of the image processing techniques with airborne geophysical data are very effective for the mineral exploration reconnaissance stages of

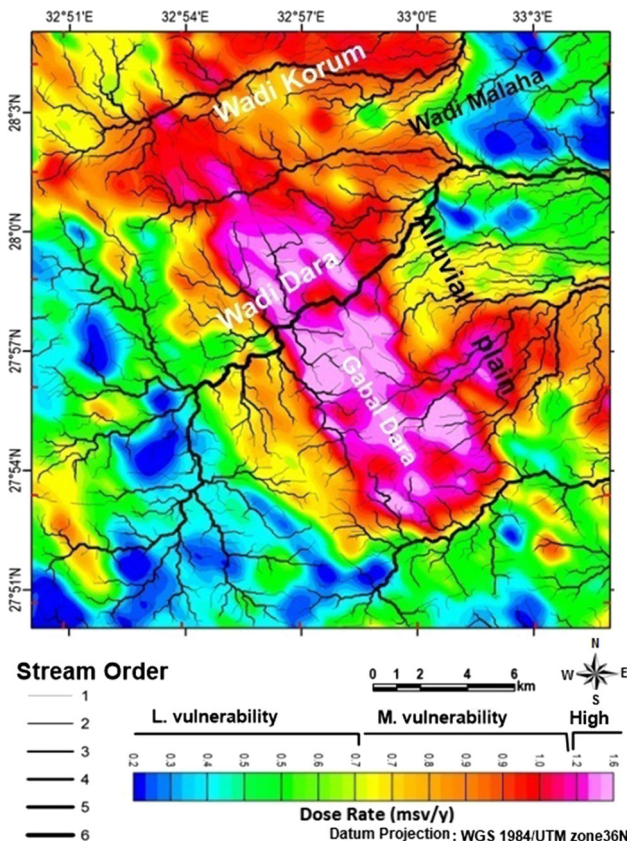


Fig. 11 Stream orders overlaying Dose rate of Gabal Dara area and vulnerability classification of the area according to the distribution of dose rates

geologists. These methods provide a quick clue in target detection and enables effective field planning. These qualities make the integration approach between the airborne methods increasingly popular for assessment of mineralization potential of the area, structural lineaments extraction, distribution of pollutants and anomaly identification. However, the accuracy of satellite-based optical remote sensing techniques and airborne data needs nearly ideal acquisition conditions such as clear weather, abundant sunlight, no land cover, and low-level-flight for gamma ray sensors.

The trend analysis of lineaments based on satellite imagery and aeromagnetic data displayed that, most of the well-developed structural lineaments have the NW–SE and NNW–SSE trends among the all maps. Therefore, these trends represent the oldest trends in the study area and could be related to hydrothermal mineralization zones. Based on these results, four favorable zones for uranium exploration have been delineated and outlined in the younger granite of Gabal Dara. These zones cannot be denied and need further ground follow-up detailed investigations. The analysis of multiple high-resolution datasets, including hyper spectral imagery and ground-based

spectroscopic surveys can confirm the presence of hydrothermal alteration in the suggested sites.

For the environmental mapping, the average dose rates in the area have been calculated from the exposure rate using the radioactive maps and range from 1.2 to 1.6 mSv/year. These values still remain in the safe side and within the maximum permissible safe natural radiation, except younger granite of Gabal Dara and the alluvial fans of the active streams. These results may be used as a reference data for monitoring possible radioactivity pollutions in future.

Acknowledgments We wish to thank Jim. Merriam, Professor of Geophysics, Department of Earth Sciences, University of Saskatchewan, Canada, and Ashraf Ghoneimi, Professor of Geophysics, Zagazig University, Egypt for their careful review of the manuscript, which has improved the accuracy of the text. We also thank reviewers for their comments, which were especially helpful in clarifying certain points in the manuscript.

References

Abd-Elmoneim HM, Shalaby MH, Salman AB (1988) Geological and beneficiation studies on Euxenite Bearing pegmatite rocks of Gabel Dara, North Eastern Desert, Egypt. In: Proceeding of the 4th conference of nuclear sciences and applications, Cairo, Egypt, Vol 1, pp 269–277

Aero-Service (1984) Final operational report of airborne magnetic/radiation survey in the Eastern Desert, Egypt for the Egyptian General Petroleum Corporation. Aero Service, Houston, Texas, April 1984, project report, six volumes

ASTER GDEM Validation Team (2009) ASTER Global DEM Validation Summary Report. METI & NASA, p 28

Berger BR, Henley RW (1989) Advances in the understanding of epithermal gold–silver deposits, with special reference to the Western US. *Econ Geol* 6(1989):405–423

Bharti R, Ramakrishnan D (2015) Exploring the unusual uranium enrichment zones in the Thar Desert, India, using remote sensing, GIS and gamma-ray spectroscopy. *Remote Sens Lett* 7(6):59–518. doi:10.1080/2150704X.2015.1051629

Boyle RW (1979) The geochemistry of gold and its deposits Geological Survey of Canada. Bulletin 1979:280

Brooknis DG (1982) Geochemistry of clay minerals for uranium exploration in the Grants mineral belt, New Mexico Mineralium Deposita March 1982, Volume 17, Issue 1, pp 37–53

Carranza EJM, Hale M (2002) Mineral imaging with Landsat Thematic Mapper data for hydrothermal alteration mapping in heavily vegetated terrane. *Int J Remote Sens* 23:4827–4852

Chiozzi P, Pasquale V, Verdoya M (2002) Naturally occurring radioactivity at the Alps–Apennines transition. *Radiat Meas* 35:147–154

Conoco and EPGC (1987) Geological map of Egypt, NF-36 NE Berince, Scale 1:500,000. Geological survey of Egypt

Crosta AP, Souza Filho CR, Azevedo F, Brodie C (2003) Targeting key alteration minerals in epithermal deposits in Patagonia, Argentina, using ASTER imagery and principal component analysis. *Int J Remote Sens* 2003(23):4233–4240

Crowley JK, Brickey DW, Rowan LC (1989) Airborne imaging spectrometer data of the Ruby Mountains, Montana: mineral discrimination using relative absorption band-depth images. *Remote Sens Environ* 29:121–134

- Cuney M (2009) The extreme diversity of uranium deposits. *Miner Depos* 44(1):3–9
- Daviz JD, Guilbert JM (1973) Distribution of radioelements potassium, uranium and thorium in selected porphyry copper deposits. *Econ Geol* 68:145–160
- El Shazly EM (1977) The geology of the Egyptian region. In: Nairn AEM, Kanas WH, Stehli FG (eds) *The ocean basins and margins*. Plenum Publishing Corporation, New York, pp 379–444
- Elsaid M, Aboelkhair H, Dardier A, Hermas E, Minoru U (2014) Processing of multispectral ASTER data for mapping alteration minerals zones: as an aid for uranium exploration in Elmissikat-Eleridiya Granites, Central Eastern Desert, Egypt. *Open Geol J* 8(Suppl 1: M5):69–83
- Feizi F, Mansouri E (2013) Introducing the iron potential zones using remote sensing studies in south of Qom Province, Iran. *Open J Geol* 3:268–278. doi:10.4236/ojg.2013.34032
- Gad S, Kusky T (2006) Lithological mapping in the Eastern Desert of Egypt, the Barramiya area, using Landsat thematic mapper (TM). *J Afr Earth Sci* 44(2):196–202
- Gad S, Kusky T (2007) ASTER spectral ratioing for lithological mapping in the Arabian-Nubian shield, the Neoproterozoic Wadi Kid area, Sinai, Egypt. *Gondwana Res* 11(3):326–335
- Ghulam A, Amer R, Kusky T (2010) Mineral exploration and alteration zone mapping in Eastern Desert of Egypt using ASTER Data. ASPRS Annual Conference, San Diego, California 26–30 April 2010
- Gupta RP (2003) *Remote sensing geology*, 2nd edn. Springer, Heidelberg, p 655
- International Atomic Energy Agency (IAEA) (2003) Guidelines for radioelement mapping using gamma-ray spectrometry data, Technical Reports Series No., IAEA-TECDOC-1363, Vienna, Austria, p 179
- International Atomic Energy Agency (IAEA) (2005) Decommissioning of nuclear facilities, IAEA safety standard series, p 27
- Javed A, Wani MH (2009) Delineation of groundwater in Kakund watershed, Eastern Rajasthan using remote sensing and GIS techniques. *J Geol Soc India* 73(2):229–236
- Loughlin WP (1991) Principal component analysis for alteration mapping. *Photogramm Eng Remote Sens* 57:1163–1169
- Matar SS, Bamoussa AO (2013) Integration of the ASTER thermal infra-red bands imageries with geological map of Jabal Al Hasir area, Asir Terrane, the Arabian Shield. *J Taibah Univ Sci* 7(2013):1–7
- Minty B, FitzGerald D (2015) Developments in airborne gamma-ray spectrometry to aid the search for strategic minerals. KEGS Symposium 2015 “Exploration for Strategic Minerals” Toronto, Canada, February 28, 2015
- PCI Geomatics (2013) Remote sensing desktop software package. Users’ Manual, Canada Center of Remote Sensing, Canada. <http://www.pcigeomatics.com/>
- Raharimahefa T, Kusky TM (2009) Structural and remote sensing analysis of the Betsimisaraka Suture in northeastern Madagascar. *Gondwana Res* 15(1):14–27
- Rowan LC, Mars JC (2003) Lithologic mapping in the Mountain Pass, California, area using advanced spaceborne thermal emission and reflectance radiometer (ASTER) data. *Remote Sens Environ* 84:350–366
- Rowan LC, Clark RN, Green RO (1996) Mapping minerals in the mountain Pass, California area using airborne visible-infrared imaging spectrometer (AVIRIS) data. In: Proceedings of the 11th conference on geologic remote sensing. Environmental Institute of Michigan (ERIM), 1
- Sabine C (1999) Remote sensing strategies for mineral exploration. In: Andrew N, Rencz et al (eds) *Remote sensing for the earth sciences*. Wiley, New York, pp 375–447
- Scheidt M, Ramsey, Lancaster N (2008) Radiometric normalization and image mosaic generation of ASTER thermal infrared data: an application to extensive sand sheets and dune fields. *Remote Sens Environ* 112:920–933
- Shalaby MH (1985) Geology and radioactivity of Wadi Dara area, North Eastern Desert, Egypt. Thesis Ph.D., Alexandria University, Egypt, p 165
- Singh A, Harrison A (1985) Standardized principal components. *Int J Remote Sens* 6:883–896
- Sroor A, El-Bahi SM, Ahmed F, Abdel-Haleem AS (2001) Natural radioactivity and radon exhalation rate of soil in Southern in Egypt. *Appl Radiat Isot* 55:873–879
- UNSCEAR (1988) Sources, effects, and risks of ionizing radiation. United Nations Scientific Committee on the Effects of Atomic Radiation 1988 Report to the General Assembly, with Annexes, p 49. http://www.uncsear.org/docs/reports/1988/1988a_uncsear.pdf. Accessed 26 Jun 2013
- Vincent RK (1997) *Fundamentals of geological and environmental remote sensing*. Prentice-Hall, Inc, Upper Saddle River, p 370
- Youssef MA, Hegab MA (2005) Using geographic information system and statistics for developing a database management system of the flood hazard of Ras Gharib area, Eastern Desert, Egypt. 4th international conference on the geology of Africa, Assiute, Egypt, Vol (2), pp 1–15
- Yu C, Cai Z, Gao Z, Zhong H (2010) Anew DEBP algorithm and its application for Hematite content predication, in computational intelligence and intelligent systems, 5th international symposium, ISICA 2010, Wuhan, China proceeding, CCIS 107, pp 11–18
- Zhang X, Pazner M, Duke N (2007) Lithologic and mineral information extraction for gold exploration using ASTER data in the south Chocolate Mountains (California). *Photogramme Remote Sens* 62:271–282